Original Research article

On the Characterization, Use and Wastewater Detoxification Potential of Pyrolysed *Moringa oleifera* Pods and Shells part A: Sorbent Preparation and Characterization.

Adams Udoji Itodo[a] *, Raymond Ahulle Wuana[a], Patience Ngunan Wombo[a,b]

a Department of Chemistry, Federal University of Agriculture Makurdi, Nigeria
b Department of Chemistry, Federal University Lafia, Nigeria

ARTICLE INFORMATION

ABSTRACT

In part A of this research, we reported adsorbent generation, characterization and optimization of factors affecting sorption. Destructive distillation technique was carried out for transforming biomass into biosorbents. Pyrolysed *Moringa oleifera* Pods **(**PMOP) and Shells **(**PMOS) were used. Adsorbents were characterized for surface morphology, crystallographic pattern, active functional sites and elemental composition using SEM, TEM, PXRD, FTIR and CHNS/O analyzer respectively. Performance assessment of adsorbent was based on removal efficiency. The effect of pH, early adsorbate concentration, contact time, adsorbent dose and temperature on chromium uptake was studied in column mode. Results show the role of both physical and chemical characteristics of the adsorbents. The maximum adsorption capacity of PMOS is 277.3 mg/g. Performance of derived sorbent compared with commercially available activated carbon shows no statistical significance at $p < 0.05$.

Graphical Abstract

*Corresponding author, email: itodoson2002@gmail.com
Department of Chemistry, Federal University of Agriculture Makurdi, Nigeria,tel:+2348039503463*
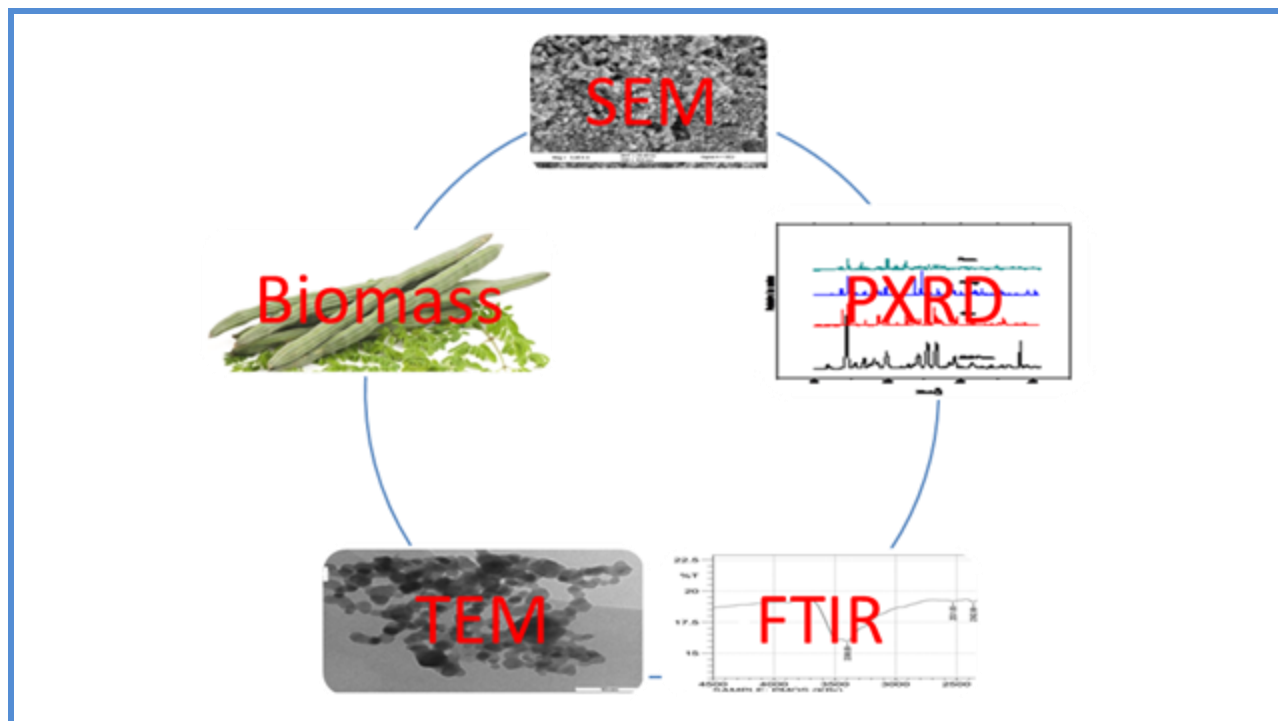
Introduction

Moringa oleifera tree identified as drumstick tree is native to India but planted around the world and found in many locales. Moringa is known for antitumor, antiepileptic, antidiuretic, anti-inflammatory and anti venomous activities. The bite characters of the plant oil have also been reported [1] The plant pigments demonstrates powerful anti-oxidative ability including vitamins C, E, A, caffeoylquinic acids, carotenoids-lutein, alpha-carotene and beta-carotene. Others are kaempferol and rutin [2-3].

Plate 1. *Moringa oleifera Seed pods and shells [4]*

Adsorbent such as active carbon available to metals wastewaters is costly and hardly available [5]. Base on this, there is a need to study the effectiveness of uptake of pollutants from tannery wastewater considering cost-effectiveness, availability and excellent adsorptive properties.

Agricultural wastes are readily available. The chemistry of Pyrolysis (destructive distillation of biomass) has been documented [6].

Amount of adsorbate adsorbed on the adsorbent (per unit adsorbent mass) is;

$$q_e = \frac{(C_0 - C_e)V}{W}$$ (1)

The modeling is of sorption capacity, deduced by measuring equilibrium concentration $C(t)$

Moringa oleifera pod had been used [7] to produce activated carbon for treating Chromium ion in wastewater. We now focus on the pyrolysis of *Moringa oleifera* waste adsorbents. Sorbent characterization was achieved with SEM, TEM, PXRD, FTIR and CHNS/O analyzer. We also report the use of absorbent for detoxification of chrome tan liquor. Performance assessment was carried out relative to those of commercial activated carbons.

Materials and methods:

AROSTEK column chromatography was used for the column studies. It has a diameter of 9-10 mm with a maximum loading capacity of 0.1 g. The elemental CHNS/O microanalysis was done by Perkin–Elmer 240C series (USA) micro-analyzer. The infrared spectra (4000-400 cm^{-1}) was performed by SHIMADZU 8400C, (Japan). Fourier transform IR spectrometer is of KBr pellets. Powder X-ray diffraction (PXRD) patterns were recorded on a BRUKER –AXS D8 Advanced X-ray Diffractometer (Germany) with Cu–Kα radiation machine at the Department of Chemistry, University of York, United Kingdom. The X-ray diffraction data were recorded using Cu Kα radiation (1.5406 A^0). The relative intensity data were collected over a 2θ range of 10–40°.

The Transmission Electron Micrograph (TEM) measurements were performed on a JEOL 1010 instruments (Japan) at 200 kV. These images were processed using Image J (1.42q) software to obtain the particle size. Scanning electron micrographs were snapped with Hitachi S-4800 microscope (Japan) at a voltage of 15 Kv. A T-60 UV-visible spectrophotometer (USA) at a resolution of 1 nm, was used to monitor the wavelength range between 200-800 nm. The chromium concentration was determined using Zenit 700 absorption spectrometer (Germany) coupled with a flame atomizer and a chromium hollow cathode lamp.

Sampling of tannery effluent

Sampling method described elsewhere [8,9] were used. Effluent samples were collected from different depths and homogenized. A clean 4L glass bottle (previously washed with 0.1 M HNO$_3$ before rinsing with distilled water) into different depths (15 cm) of the effluent was lowered and allowed to overflow with effluent before withdrawal. The bottle was sealed before storing at 4 ^{0}C till required for further analysis. Temperature, total dissolved solids, pH and conductivity were

determined *in situ*. The effluent sample was treated with HNO_3 (conc.). Method of effluent preservation was as described [10-12].

Sampling and preparation of precursors

Moringa oleifera seeds were obtained from the Central Market in Lafia, Middle-Belt Nigeria. The *Moringa oleifera* seeds pods and shells were taken for identification at the Botany Department of the University of Agriculture Makurdi, Nigeria. The seed pods were deseeded, deshelled and washed with water to remove dust, sand and allowed to dry at room temperature. The seed pod was pounded in a mortar using a pistol and further blended to a coarse size (1 mm diameter).

Preparation of adsorbents

A method used by Ahmedna *et al.*[13] was followed. Dry sample (100 g) was finely crushed in a mortar using pestle until all particles are separated then further blended using a blender and sieved using a 200 um sieve size.

Pyrolysis of adsorbents

A documented method [14] was adopted for pyrolysis. The *Moringa oleifera* seed pods and shells were washed with tap water followed by distilled water, to remove dirt and air-dried. The shell and pod, 160 g and 150 g respectively were placed in a muffle furnace and heated at a rate of $400\ ^0C$ for 8 hours. The washed activated sample was dried in an oven at 105^0C to constant weight. Adsorbents were kept in an airtight polyethene bag [15], labelled and stored for further analysis.

Digestion of effluent for AAS analysis

Digestion method by Edgell [16] was adopted; 10 mL of 1:1 HNO_3 was added and mixed with the 2 mL of the tan-chrome effluent and cover with a watch glass. The sample was heated to $95\ ^oC \pm 5^o$ C and reflux for 10 to 15 minutes without boiling. It was allowed to cool. 5 mL of concentrated HNO_3 was added. The mixture was covered with a watch glass and refluxed for 30 minutes. Brown fumes indicate oxidation of the sample by HNO_3. Digestion was repeated (with the addition of 5 mL of conc. HNO_3) until no brown fumes were given off. After cooling, 2 mL of water and 3 mL of 30% H_2O_2 was added. The vessel was covered with a recovery device and returned to the heat source for peroxide reaction. The heat was applied until effervescence subsided and the vessel cooled.

Heating of the acid-peroxide digest continued until the volume was reduced to approximately 5 mL. 10 mL of concentrated HCl was added to the digest and covered with a watch glass. The tan-chrome was then placed on/in the heating source and reflux at $95\ ^of \pm 5\ ^oC$ for 15 minutes. The digest was

filtered using a Whatman No. 41 and the filtrate collected in a 100 mL volumetric flask. The effluent digest was diluted to the mark and analyzed for chromium using AAS.

Characterization of Adsorbents

The adsorbents were characterized for pH, bulk density, moisture content, loss on ignition (LOI) and iodine adsorption number. Instrumental characterization includes Fourier transform infrared (FT-IR), Scanning Electron Microscope (SEM), Thermal Electron Microscope (TEM), Ultraviolent-visible spectroscopy, X-Ray Powder Diffraction Analysis (XRD) and CHNS/O elemental analysis.

Adsorbent pH: a Standard test method for pH (ASTMD3838-80) was adopted. 1.0 g of adsorbents were weighed separately and transferred into beakers. 100 mL of distilled water was measured, added and stirred for 1 h. The samples were allowed to stabilize before the pH was measured using a pH meter. Samples will be run in triplicates and values recorded.

Bulk density: The procedure described by Banerjee and Chattopadhyaya was used [17]. The pre-weighed specific density bottle filled with distilled water was weighed. The bottle was then filled with the adsorbents and weighed. Bulk density was computed as:

$$Bulk\ density\ = \frac{W_2 - W_1}{V}\ \text{(g cm}^{-1}\text{)} \qquad (2)$$

Where W_1 = weight of the empty bottle, W_2 = weight of empty bottle and adsorbents, $W_2 - W_1$ = weight of adsorbents, V mL = Volume of the adsorbents or Volume of water needed to fill the bottle.

Moisture content: The method used by Toles *et al.[18]* was adopted, the beaker containing adsorbents with moisture was weighed. Then oven dried, powdered adsorbents weighed followed by overnight drying at 80⁰ C in the oven until a constant weight was reached

$$\text{Moisture content (\%)} = \frac{Mass\ of\ water}{over - dry\ mass}\ x\ 100 \qquad (3)$$

Particle size: Estimation of particle size of the adsorbents was from particle distribution in TEM images. The images were analyzed using image j software [19]. 250 g of the dry sample was finely crushed in a mortar using pestle until all particles are separated. The sieve was then installed according to the size together with the receiver and cover. 200 g of the sample sieved using the British standard sieve. The sample was pulverized and sieved using the 150 μm sieve size before SEM micrography.

$$\text{\% Retained} = \frac{W_{seive}}{W_{total}}\ x\ 100 \qquad (4)$$

Loss on ignition (LOI): In estimating LOI [21], the dried sample was ground and put in the crucibles and transferred to the furnace for ignition at 400 ⁰C for 5 hours. The weight of each

adsorbent was measured before and after ignition. Loss on ignition (LOI) was estimated by difference.

Iodine adsorption number: For the iodine number test [21], 100 mL of the stock iodine solution was added and agitated at a fast speed, using an electric shaker for a period of 60 min. The mixtures were filtered through a sintered glass crucible. An aliquot portion of 20 mL was titrated with 0.1 M sodium thiosulphate using starch as an indicator. The concentration of iodine adsorbed by the adsorbents at room temperature was calculated as the amount of iodine adsorbed in mg.

$$\frac{Img}{g} = \frac{(B-S)}{B} \; x \; \frac{VM}{M} \; x \; 253.81 \qquad (5)$$

where, B and S are the volumes of thiosulphate solution for the blank and sample titrations, respectively. W is the mass of the adsorbents, M is the concentration (mol) of the iodine solute, 253.81 is the atomic mass of iodine and V is 20 mL aliquot.

FTIR Characterization: Fourier transform infrared (FT-IR) spectroscopic analysis was used to study the surface chemistry of the surface modified *Moringa oleifera* seed pod and shells. The FT-IR spectra of the absorbents before and after adsorption of the tan-chrome liquor were recorded.

SEM Characterization: Scanning electron microscopy was used to study the morphology of the surface modified *Moringa oleifera* seed pod and shell. The SEM images of the absorbents before and after adsorption of the tan-chrome liquor was recorded. The Scanning Electron Microscope (SEM) images of the virgin adsorbents, effluent loaded and chemically regenerated activated carbon at selected magnifications was observed. The micrograph displays the surface structure or morphology of the adsorbent. This was carried out using SEM equipment (SEM, model: Phenomenon Prix, MVE016477830).

TEM Characterization: Thermal electron microscopy was used to study the morphology of the surface modified *Moringa oleifera* seed pod and shell. The TEM images of the absorbents before and after adsorption of the tan-chrome liquor was recorded.

XRD Characterization: X-ray diffraction (XRD) is a material characterization technique that can be useful for analyzing the lattice structure of a material.

CHNS/O elemental analysis: A CHNS/O is a scientific instrument which can determine the elemental compound of a sample. The names derive from the four primary elements measured by the device Carbon (C), Hydrogen (H), Nitrogen (N), Sulphur (S) and Oxygen (O). The analyser uses a

combustible process to break down substances into simple compounds which are then measured by separating out inorganic carbon using a solvent.

Description and Preparation of column

A Rostek column Instrument with diameter 9-10 mm and Max loading of 100 mg (0.1g) was used. The column was clamped on a retort stand vertically; the raw tannery effluent was poured from the top while the treated effluent was collected from the tap.

The column was washed with distilled water and dried in an oven. A piece of cotton was introduced into the glass column close to the tap to ensure adsorbents do not block the column. The desired weight of the adsorbents was then weighed (bed depth) and carefully placed in the column, with continuous tapping to remove trapped air. The set up was wet with distilled water and set for use.

Adsorption Experiments

Method for sorption experiments [21] was adopted. The adsorbents were packed into the vertical column to obtain the bed depth, and the column was tapped to remove air bubbles. The applied shaking (1000 rpm) speed allows all the surface area to come in contact with heavy metal ions over the course of the experiments. All experiments were carried out in duplicate. The effect of various parameters on the rate of adsorption process was observed by varying contact time, adsorbate concentration, temperature, adsorbent dosage and pH of the solution. The solution volume was kept constant [23]. The pH of the effluent solution was determined with the aid of a pH meter. The flasks were plugged with foil paper and kept closed to avoid the fluctuation of pH due to the exchange of gases during the experiment.

Optimization of Parametric Factors

For optimum working condition, the effect of pH, initial concentrations, temperature and dosage were investigated.

Effect of initial concentrations of adsorbates

According to a method by Kilic, *et al.*[24] , five initial concentrations (200, 400, 600, 800, and 1000 mg/L) were used. Kept constants are; pH 6; 30 ± 2°C, 0.05 g, 0.025 dm^3 and 60 minutes. At the end of each period outflow of the eluate was collected in sample bottles, labelled and stored for analysis.

Effect of temperature

Effect of temperature [25] was estimated by varying the temperature of the Tan-chrome liquor (10, 20, 30, 40, and 50^{0}C) all other parameters kept constants. The eluate was collected in sample

bottles, labelled and stored for analysis. The constancy of the temperature was maintained with an accuracy of ± 0.5 ºC.

Effect of pH

The pH of the Tan-chrome liquor was varied as; 2.0, 4.0, 6.0, 8.0, and 10.0. At the end of each period outflow of the eluate was collected in sample bottles, labelled and stored for analysis [24].

Effect of contact time

A method earlier reported [26] was used. This involves varying the contact time of the Tan-chrome liquor with the adsorbents from 20 min, 40 min, 60 min, 80 min and 100 min. After each period outflow of the eluate was collected in sample bottles, for analysis.

Effect of adsorbent dosage

A method [24] was adopted; this was carried out by varying the adsorbent dose (0.01, 0.02, 0.03, 0.04, 0.05 g). Eluate was collected in sample bottles for analysis.

Test of significance was achieved using One-way Analysis of Variance (ANOVA) at 95% confidence limits to compare adsorptive properties of the adsorbents with those of standard commercial activated carbon (CAC).

Results and Discussion

Visual Inspection and Yield of Adsorbents: Physical appearance of the adsorbent as well as the percent yield of adsorbents was reported in Table 1. The adsorbents has similar appearance after modification. PMOS is black crystalline in appearance and has a yield of 17.6%. PMOP also appeared black crystalline with a yield of 22% while the spent adsorbents were dark brown colours

Table 1. Percentage yield and appearance of adsorbents

Adsorbents	Appearance	Yield (%)
PMOS	Black crystalline	17.6
PMOS	Black crystalline	22.0

Elemental composition of adsorbents: The CHNO/S analysis (Table 2) showed that all the samples where nontoxic. Carbon percentage was as follows: CAC; 88.75, PMOS;49.98 and PMOP is 39.05%.

Table 2. Comparative elemental composition of adsorbents derived from *Moringa* seed pods and shells

S/no	Elements	Composition (%)		
		PMOS	**PMOP**	**CAC**
1.	Carbon (%)	49.98	39.05	88.75
2.	Hydrogen (%)	<1.00	<1.00	<1.00

3.	Nitrogen (%)	<1.00	<1.00	<1.00
4.	Sulphur (%)	ND	<1.00	<1.00
5.	Oxygen (%)	0.22	0.14	1.07

ND- Not detected

Hydrogen compositions (%) was estimated as <1% for CAC, PMOS and PMOP. Nitrogen and sulphur compositions were equally < 1% for CAC, PMOS and PMOP. It was opined that traces of hydrogen and nitrogen elements were traced to herbaceous impurities [30]. Oxygen percentage was 0.14 for PMOP, PMOS; 0.22 and CAC gave 1.07%. The elemental composition of PMOS and PMOP when compared to CAC are in close range, this could be attributed to nearness in carbonization and activation temperature for both adsorbents.

Physiochemical Parameters of the Adsorbents: Results of the physicochemical parameters of adsorbent was reported as mean value and presented in Table 3.

Table 3. Physicochemical properties of the adsorbents

s/no	Parameters	PMOP	PMOS	CAC
1.	pH	7.18	7.02	7.02
2.	Bulk density (g/cm³)	5.62±0.02	4.20±0.02	0.10±0.02
3.	Moisture contents (%)	2.83 ±0.02	2.40 ±0.02	1.02±0.02
4.	Surface area (m²/g)	220.10±0.02	280.17±0.02	520.66±0.02
5.	Particle size (um)	24	19	9.0
6.	Iodine adsorption number	180.34±0.02	218.02±0.02	354.65±0.02
7.	Loss on Ignition	22%	17%	ND

ND= Not detected

pH of **Adsorbent** is an important parameter applied in adsorbents production. pH above or below the acceptable limit will have an effect on the material to be adsorbed. The acceptable limit for pH is 6.5 to 7.5. The pH of adsorbents, PMOS stands at 7.02; PMOP is 7.18 and CAC at pH7.02.

Bulk density: The bulk densities of the adsorbents are PMOS; 4.20, PMOP; 5.62 and CAC; 0.12. g/cm³. Bulk density is observed to be lesser for CAC compared to pyrolysed adsorbents.

Moisture content can be said to be a measure of the amount of water (in any form) in a material, substance or adsorbent at any given time. Moisture content was reported for PMOS as 2.40%, PMOP as 2.83% and 1.01% for CAC. Moisture content is observed to be highest in the PMOP. This may be due to the toughness of the sample material which enhances its inability to expel moisture as the other samples at the experimental temperature.

Particle size was determined using Image J software on the particle distribution of the SEM images. The results are PMOS; 0.83 um, PMOP; 1.45 um and CAC; 0.65 um.

The surface area of any solid is an estimate of the entire area occupied by the object. Surface area finds application in chemical kinetics. The higher the surface area of a substance, the more the active site and subsequently high reaction rate are. For different applications, optimization of surface area is a good practice. Surface area for PMOS is 280.17 m^2/g, PMOP is 220.10 m^2/g and CAC is 520.66 m^2/g.

Iodine adsorption number is useful in characterizing carbon blacks. The presence of volatiles, surface porosity, or extractable will influence the iodine adsorption number. Ageing of carbon black can also influence the iodine number. Adsorbents with high iodine number perform better in removing small sized contaminants. It is the most fundamental parameter used to characterize the performance of activated carbon. A high value indicates a high degree of activation [27-29]. Iodine adsorption number for the PMOS is 218.02; PMOP is 180.34 and CAC 354.65, indicating the suitability of the adsorbents under consideration in the removal of micro size adsorbates (such as toxic metals) from the aqueous medium.

Volatile matter refers to components of a substance other than moisture, which is liberated at high temperature in the absence of air. It comprises of short and long-chain hydrocarbons, aromatic hydrocarbon and sulphur. Volatile matter measures the level of gaseous fuels present in the biomass. The volatile matter for the PMOS is 9%, PMOP is 7 % and CAC is 12 %. This follows the trend of PMOP< PMOS<CAC.

SEM Characterization: The surface morphology of the adsorbents was studied by scanning electron microscopy. Plate 2 shows micrographs of PMOS; PMOP (pyrolysed shell and pod). Also presented were SEM images for CAC and spent PMOS. The SEM images were used to investigate the surface morphologies of the adsorbents. The materials displayed uniform (homogeneous) structure. The micrograph of PMOS shows a non-homogenous and rough surface with interspaces which are presumably pored [30]. The micrograph of PMOP also appeared as rough, tiny interspaced structures. Plate 2H images show the adsorbed tannery effluent onto the adsorbent (PMOS), depicting surfaces occupation by particles after adsorption, it is clearly observed that the caves, pores and surfaces of adsorbent were covered by adsorbates consequently rendering the surface to become smooth.
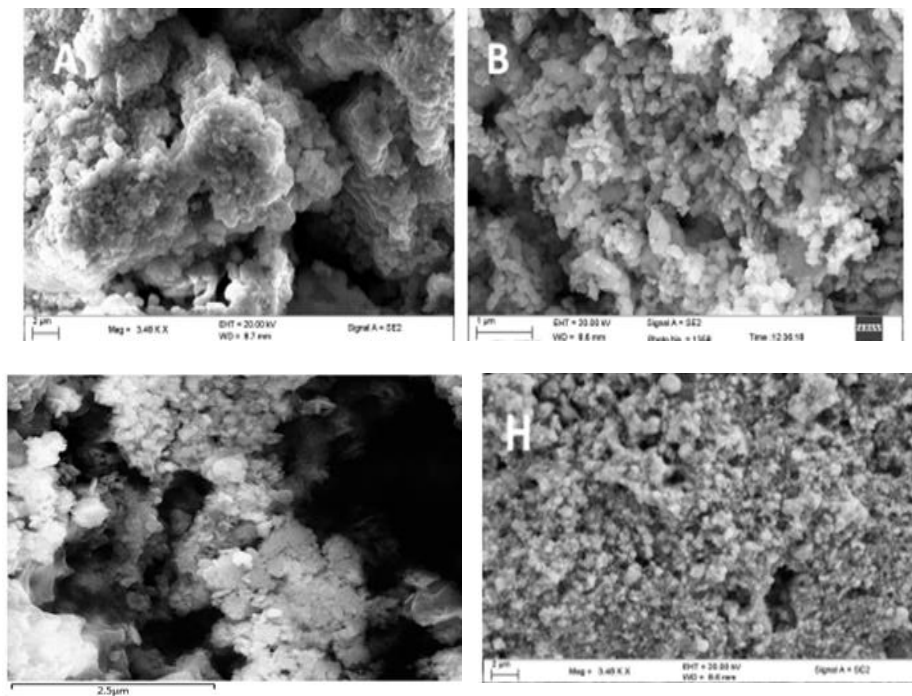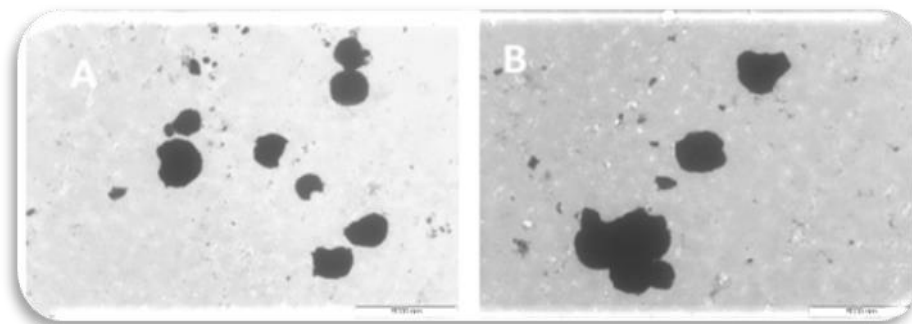
Plate 2. SEM images of PMOS (A); PMOP (B); CAC and spent PMOS (H)

TEM characterization: The microstructural morphology of the adsorbents was studied using transmission electron microscopy. Plates 3A and B show micrographs of PMOS and PMOP. TEM images for CAC (commercial activated carbon) and Spent PMOS (Pyrolysed shell) were presented also presented. Image J distribution of the particles gave mean sizes as follows; PMOS (0.83 um), PMOP (1.46 um).
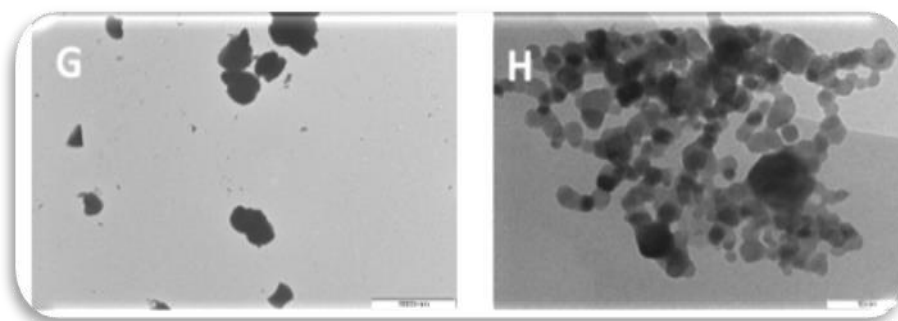
Plate 3. TEM images of PMOS (A); PMOP (B); CAC (G) and Spent PMOS (H)

FT-IR Characterization: Fourier transform infrared (FT-IR) spectroscopic analysis was used to study the surface chemistry of the pyrolysed *moringa oleifera* seed pods and shells. It can be seen from Figure 1 that the FT-IR spectrum of each absorbent have different frequencies from the other, in that there was a significant change in structure upon pyrolysis of shell and pods at 600 °C. The high intensity and sharp peaks observed in the adsorbents may be due to the highly crystalline nature of the products. The FT-IR spectra of the raw biomass showed broad bands at a range of 3446-3281 cm^{-1} corresponding to -OH and –COOH stretching vibration frequencies [31]. However, a disappeared band in the pyrolysed products (PMOS, PMOP and CAC) is due to escape of organic functional groups via volatilization. All the adsorbents exhibited vibration frequency at 350-750 for -C-H; 750-1250 for either C-O stretch, CH$_2$ symmetric deformation, C≡C stretch and C=C stretch.
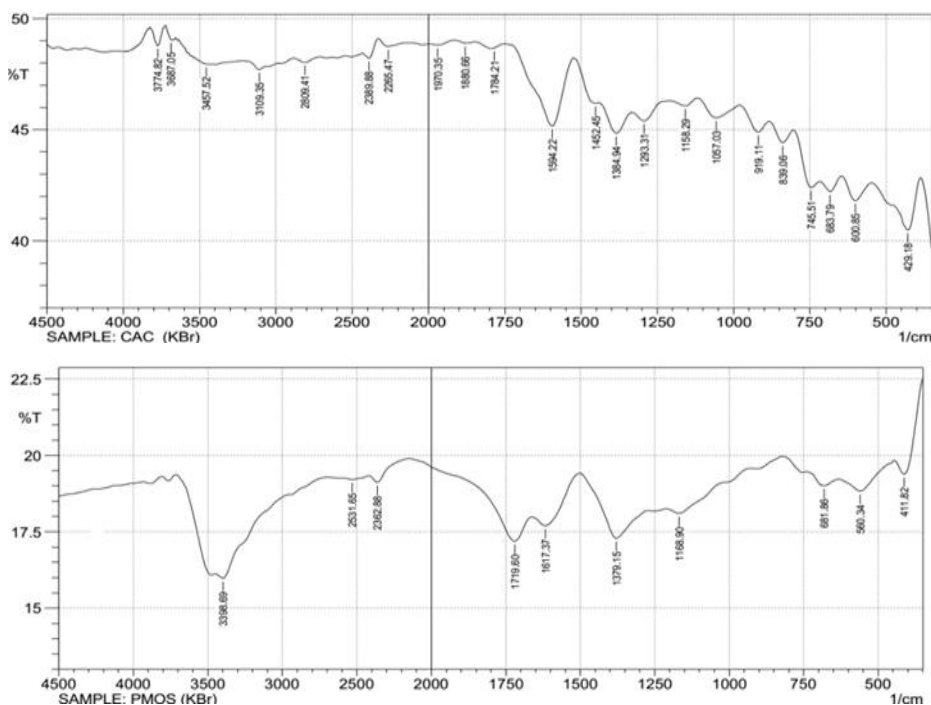

Figure 1. FTIR Spectra of CAC and PMOS

PXRD Diffraction Pattern of the Adsorbents: X-ray diffraction (XRD) as a non-destructive analytical technique is a material characterization technique that is useful for analyzing the lattice structure of a material system. It unveils crystalline properties of a material. The XRD for the adsorbents is presented in Figures 2. Low and high-intensity diffraction peak was observed for the adsorbents. There was a complete collapse of adsorbents on the spent (Cr-PMOS). This could be due to a decrease in the crystalline nature of the material after adsorption [31].The X-ray diffraction (XRD) analysis of PMOS, PMOP and CAC showed peaks that indicate crystalline structure diffraction peaks while the spent PMOS showed amorphous peaks, indicating changes in the surface structure after adsorption [32]. Crystallographic parameters of the adsorbents are presented in Table 4.

Table 4. Crystallographic parameters of adsorbent

Adsorbents	Peak position 2θ (degree)	Full width at half maximum intensity (FWHM) ß (rad)	d-spacing	Crystalline /D (um)
PMOS	13.83	112.82	6.3976	0.0123
	16.40	763.73	5.3992	0.00183
	18.78	235.09	4.7211	0.00597
	19.95	1000.00	4.4472	0.00140
	22.33	79.74	3.9790	0.0177
	25.43	23.63	3.4993	0.0601
	30.21	237.45	2.9564	0.00604
	34.98	268.75	2.5633	0.00540
PMOP	18.52	716.74	4.7861	0.00195
	22.42	1000.00	3.9616	0.00141
	23.93	555.43	3.7158	0.00255
	25.69	942.90	3.4648	0.00150
	26.58	615.30	3.3506	0.00231
	31.71	231.15	2.8195	0.00623
	38.42	103.10	2.3410	0.0142
	44.36	146.90	2.0403	0.0101
	45.06	19.40	2.0105	0.0773
CAC	15.16	1000.00	5.8406	0.00139
	17.38	167.71	5.0998	0.00836
	18.70	847.28	4.7409	0.00165
	26.05	38.21	3.4182	0.0372
	38.24	612.66	2.3515	0.00239
	44.62	222.86	2.0292	-0.0847

From the results CAC had 6 prominent peaks with 2θ ranging from 15.16 to 44.62, PMOS (8 peaks with 2θ from 13.83 to 34.98); PMOP (9 peaks with 2θ ranging from 18.52 to 45.06)**.**
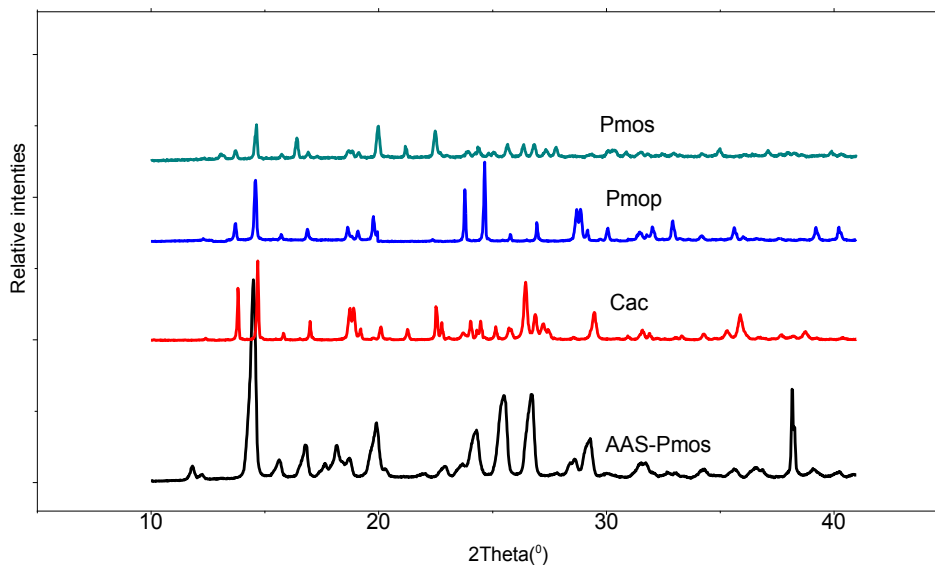

Figure 2. PXRD pattern for PMOS, PMOP, CAC and Spent PMOS

## Optimization of Adsorption Parameters

Parametric factors such as initial concentration, pH, time and temperature were monitored in order to optimize the working parameters (Figure 3).

Effect of initial metal concentration: The adsorption performance by the absorbents was evaluated as an initial chromium concentration (200 – 1000 mg/L), pH value of 6, 30 ± 2ᵒC, 0.05 g adsorbent dose and 60 minutes adsorbent/adsorbate contact time. Cr absorptive (quantity removed and percentage adsorbed) increased with the increase in the initial metal concentration until peaks were reached. The trend is linked to an increase in driving force of the concentration gradient. Comparatively, results show that the percentage of heavy metals adsorbed on the adsorbents were in the order of PMOP < PMOS for chromium. The effect of the initial concentration depends on the immediate relationship between the heavy metal concentration and the available binding sites on an adsorbent surface [33]. The optimum quantity of chromium adsorbed was found to be 120.444 mg/g and 232.876 mg/g for PMOP and PMOS respectively. The higher quantity of chromium adsorbed on PMOS than on PMOP is attributed to the large surface area and higher pore volume of PMOS [34].

Effect of adsorbent Dosage: Removal efficiency increased with increase adsorbent dose. For a fixed early adsorbate concentration, increasing adsorbent dose provides greater surface volumes

(more adsorption sites), creating sites for contacts. For chemisorption, there is an increase in electrostatic interaction at the sorbate-sorbent boundary. The higher the electrostatic interaction between the adsorbent and the metal ions, the higher the metal uptake level [35]. Results from this studies show that the percentage of chromium adsorbed on the absorbents, the pyrolysed absorbents still upheld higher adsorption capacities as compared to the unpyrolysed absorbents. The order was as follows; PMOP < PMOS for chromium, within the studied range of the adsorbent dosage.

Effect of temperature on adsorption: The absorptivity peak was reached for the adsorption of chromium at 30°C. The increased adsorption with a rise in temperature may be diffusion controlled, which is an endothermic process i.e. the rise in temperature favours the transport of the adsorbate within the pores of the adsorbent. Further increase in temperature caused a proportional decrease of the metal ions adsorbed onto the surface of the adsorbent. This may be attributed to the weakening of the attractive forces between the adsorbent and the adsorbate induced by the further rise in temperature [36]. At high temperature, a thickness of boundary layer decrease due to the increasing tendency of metal escape owing to the increase kinetic energy [37]. The observed adsorption trend with temperature is as follows; PMOP < PMOS for chromium uptake.
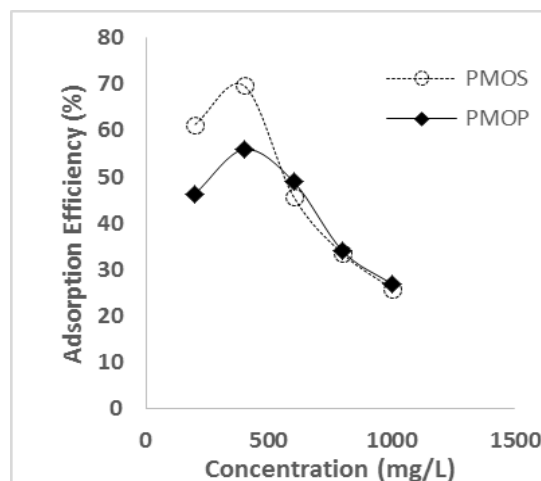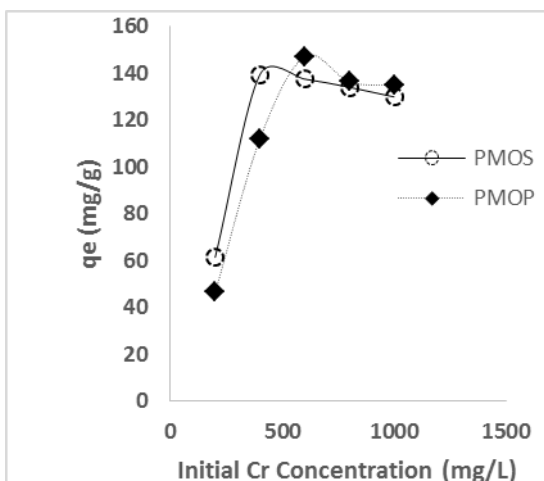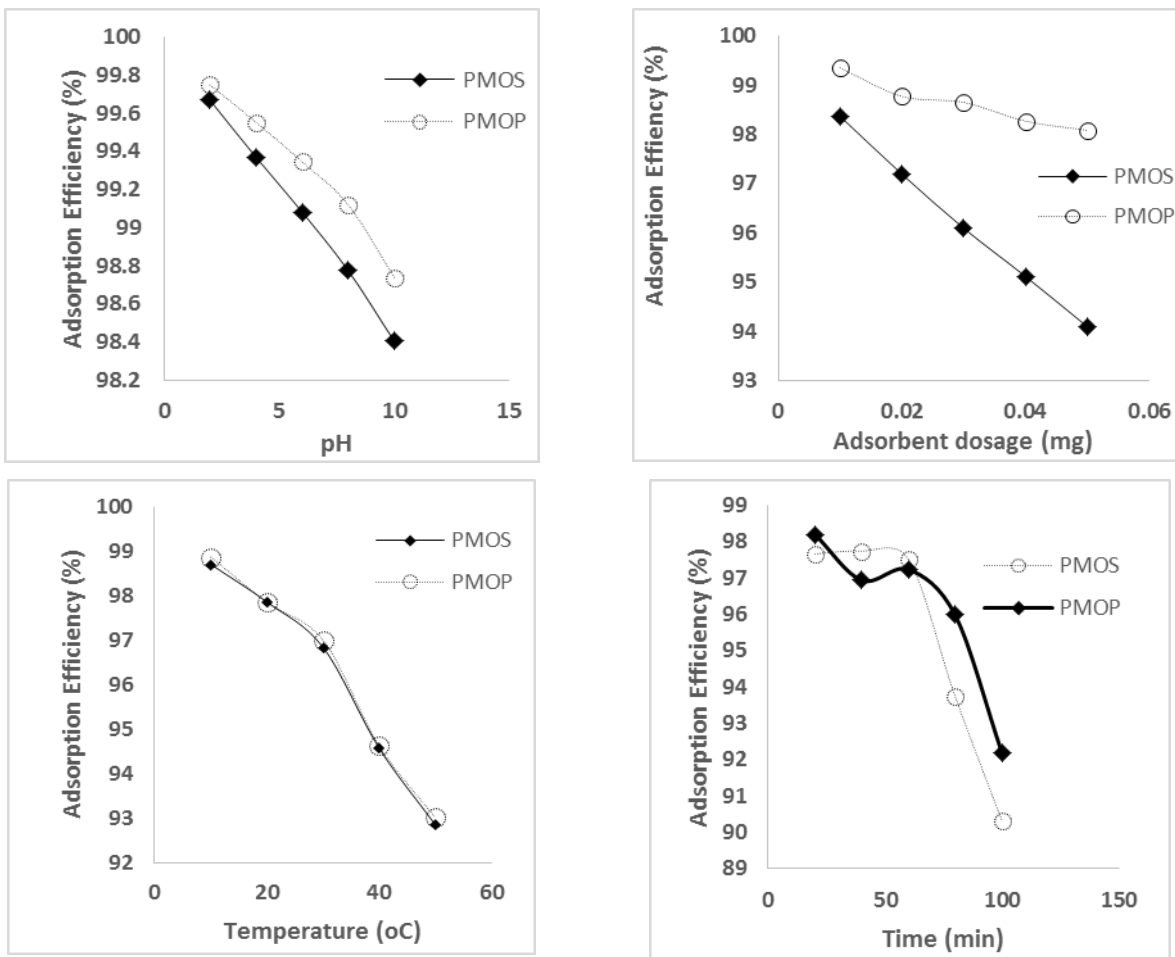
Figure 3. Effect of Parametric factors; Initial Cr Concentration, pH, Dosage, Temperature and Contact time

Effect of pH on adsorption: The adsorption behaviour of Chromium ion was studied from the aqueous solution at different pH values. The pH is one of the principal factors influencing the adsorptive capacities of metal ions. The pH of the solution was varied from 2 to 10. Results show that the pH for optimum adsorption of chromium ions for PMOS is pH 6, PMOP is pH 8 and CAC is pH 6. Similar trends were reported [34,38]. The increase in the amount of metal ion adsorbed at this pH may be explained on the basis of a decrease in competition between proton (H^+) and the positively charged metal ion at the surface sites. A decrease in positive charge near the surface results in a lower repulsion of the adsorbing metal ion. When alkalinity increased that is from pH value of 9 to 10, there was further decrease in the rate of adsorption by adsorbents for chromium ions in aqueous solution. This could be as a result of the decrease in the degree of protonation of the adsorbent functional group [39].

Effect of contact time on adsorption: The effect of contact time on adsorption of chromium ions was studied at pH 6, 30 ± 2°C, 0.05 g adsorbent and concentration 400 mg/L. With an increase in contact time (10 to 100 minutes) chromium removal was increased. It was observed from the study that the adsorption of chromium on the adsorbents increased with increase in contact time until equilibrium was reached at 60 mins. Maximum chromium removal was observed at 60 minutes for PMOS, 80 minutes for PMOP, while CAC was 40 minutes.

Conclusions

Absorbents derived from *Moringa oleifera* seed shells and pods were successfully prepared, characterized, utilized and compared for their sorptive properties with those documented in literatures and with the commercially available activated carbon. The comparable level of percentage removal using the adsorbents is an indication of the potential applicability of the pyrolysed *Moringa oleifera* adsorbents. The highlight of their sorptive properties was presented as "PART B" of the same title[40].

References

[1]. Hsu R., Midcap S., Arbainsyah D., Witte L. *National Herbarium*, Leiden, 2006

[2]. Ho S.Y., McKay G. *Canadian Journal of Chem. Eng.,* 1994, **76**:822

[3]. Aslam M.F., Anwar R., Nadeem U., Rashid T.G., Kazi A., Nadeem M. *Asian Journal of Plant Science*, 2005, **4**:417

[4]. Healthline , Healthline Bulletin, 2005.

[5]. Demirbas E., Kobya M., Sulak M.T. *Bioresources Technology*, 2008, **99**:5368

[6]. Itodo A.U., Abdulrahaman F.W., Hassan L.G., Maigandi S.A., Hapiness U.O., *Iranian Journal of Chemistry and Chemical Engineering, 2011,* **30**:51

[7]. Abdulrazak S., Sulyman Y.I, Bello H.I. Bello, Akanni A.S., Oniwapele Y.A., Muktari M. *Journal of Environmental Science, Toxicology and Food Technology ,* 2015, **9**:96

[8]. Kawse A.M., Monika D., Islam M.M., Mosammat S.A., Shahidul I., Muhammad A.A-M. *World Applied Sciences Journal, 2011,* **12**:152

[9]. Islam B.I., Musa A.E., Ibrahim E.H., Salma A.A.Sh., Babiker M.E. *Journal of Forest Products & Industries, 2014,* **3**:141

[10]. APHA American Public Health Association, American Water Works Association, and Water Environment Federation, Washington, DC.

[11]. Freeman N.D., Pardon K.K.., Edison M., Mohammed B. *Proceedings of the World Congress on Engineering and Computer Science-WCEC (1)*, San Francisco, USA., 2009

[12]. Reeve R.N., *Introduction to Environmental Analysis*, John Willey and Sons, Limited, Chichester, England, 2002,p 112.

[13]. Ahmedna M., Marshall W.E, Rao R.M. *Bioresource Technology*, 2000, **71**:113

[14]. Adowei P., Horsfall M., Spiff A.I. *Innovation Science Engineers,* 2012, **2**:24

[15]. Tarawou T., Horsfall M., Jose V.L. *Chemistry Biodiversity,* 2007, **4**:2236

[16]. Edgell K., . USEPA, 1988 No. 68-03-3254.

[17]. Banerjee S., Chattopadhyaya M.C. *Arab Journal of Chemistry*. 2013

[18]. Toles C.A., Marshall W.E., Johns M.M., Wartelle L.A., McAloon A. *Bioresource Technology*, 2000, **71**:87

[19]. Al-Ghouti M.A., Khraisheh M.A.M., Allen S.J., Ahmad M.N. *Journal of Environmental Management,* 2003, **69**:229

[20]. Demirbas A. J*ournal of Hazard Materials ,* 2009, **167**:1

[21]. Ramuthai S., Nandhakumar V., Thiruchelvi M., Arivoli S., Vijayakumaran V., *E-Journal of Chemistry*, 2009, **6**(S1):S363

[22]. Gimba C., Musa I., *Journal of Chemical Nigeria,* 2007, **32**:167

[23]. Mulu B. *Journal of Thermodynamics*, 2013, **6**:1

[24]. Kilic M., Apaydin-Varol E., Pu¨tu¨n A.E. *Journal of Hazard Materials,* 2011, **189**:397

[25]. Gueu B.S., Yao K., Adouby G.A. *International Journal of Environmental Science and Technology*, 2007, **4**:11

[26]. Vaishali T., Dinesh K., *Chemistry Central Journal, 2013,* **7**:1

[27]. Aziza A., Odiakosa A., Nwajei G., Orodu V. Proceeding. *Chemical Society of Nigeria*. Deltachem 2008, 235.

[28]. Elliott C., Colby T., Iticks H. *Chest.,* 1989, **96**:672

[29]. Itodo A.U., Abdulrahman F.W., Hassan L.G, Maigandi S.A., Itodo H.U. *New York Science Journal,* 2010, **3**:17

[30]. Nor S.A, Mohd H.H, Syazrin S.S., Muhammad A.M.F. *Sci.Int.*, 2017, **29**:7

[31]. Chen J.J., Chen Y.T., Raja. D.S., Kang Y.N., Tseng P.C., Lin C.H., *Materials*, 2015, **8**:5336

[32]. El-Trass A., Elshamy H., El-Mehasseb I., El-Kemary M. *Applied Surface Science*, 2012, **258**:2997

[33]. Akhtar S., Qadeer R. *Turk. J. Chem.*, 2005, **29**:95

[34]. Onwu F.K. *Afr. J. Biotechnol.*, 2010, **9**:7086

[35]. Brinda L., Rajan K.S., Rayappan J.B.B. *Journal of Applied sciences*, 2012, **12**:1778

[36]. Abbasi A.R., Akhbari K., Morsali A. *Ultrason. sonochem*, 2011, **19**:846

[37]. Saleh T.A., Gupta V.K., *J. Colloid Interface Sci.*, 2012, **371**:101

[38]. Egila J.N, Dauda B., Jimoh T. *Afr. J. Biotechnol.*, 2010, **9**:8192

[39]. Ajmal M., Rao R.A., Ahmad K., Ahmad R. *J. Hazard. Mater*. 2000, **79**:117

[40]. Itodo A.U, Wuana R.A., Wombo N.P., *Chemical Methodologies,* 2018, **2**:171